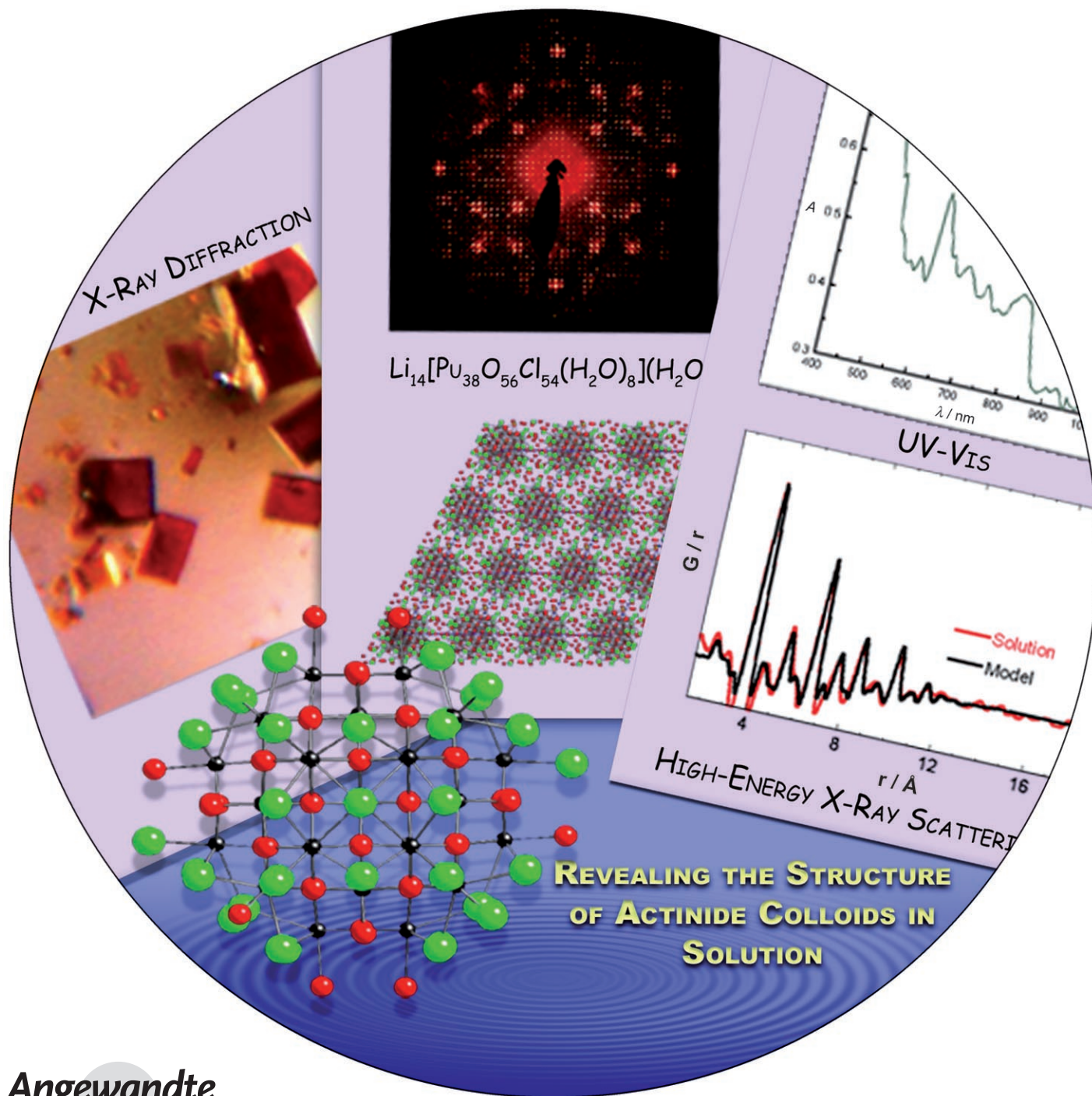


# The Structure of the Plutonium Oxide Nanocluster

## $[\text{Pu}_{38}\text{O}_{56}\text{Cl}_{54}(\text{H}_2\text{O})_8]^{14-} \cdot \cdot$

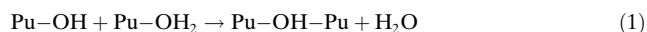
*L. Soderholm,\* Philip M. Almond, S. Skanthakumar, Richard E. Wilson, and Peter C. Burns\**



The aqueous solution chemistry of tetravalent plutonium is typical of a small, highly-charged metal ion. Under all but very acidic conditions, Pu<sup>IV</sup> undergoes hydrolysis with products that further react to form multinuclear metal oligomers. These aggregates are thought to be complex hydroxides and hydrous oxides<sup>[1,2]</sup> that can persist in solution indefinitely and, upon aging under select conditions, form chemically ill-defined precipitates, which for the case of Pu<sup>IV</sup> resemble poorly crystalline PuO<sub>2</sub>. We have characterized metal complexes from solutions exhibiting the classic intractable chemistry of hydrolyzed Pu, and instead of ill-defined hydrous oxides, we find monodisperse, nanometer-sized, surface-stabilized particles of the dioxide. Diffraction studies of single crystals formed from these solutions reveal well-defined nanoclusters of [Pu<sub>38</sub>O<sub>56</sub>Cl<sub>54</sub>(H<sub>2</sub>O)<sub>8</sub>]<sup>14-</sup>. The precipitation of such well-defined, monodisperse oxide clusters suggests a similarity with the hydrolysis chemistry seen for hexavalent d-block ions such as tungsten and molybdenum, which are known to form a wide variety of well-defined iso- and polyoxometalates.<sup>[3]</sup>

In the laboratory, the presence of Pu<sup>IV</sup> colloid is operationally defined by the ineffectiveness of standard ion-exchange and solvent-extraction separations together with a characteristic optical spectrum.<sup>[4]</sup> Well-studied because of its impact on Pu solution chemistry, colloid, or “polymer”, formation occurs even at low pH values and low concentrations and has recently been demonstrated to account for the large discrepancy in measured solubility constants of Pu.<sup>[5,6]</sup> In large-scale chemistry associated with nuclear waste reprocessing, the formation of hydrolysis products vitiates current separations scenarios,<sup>[7]</sup> while in the geosphere, colloid formation is believed to be responsible for the facile Pu groundwater transport observed at contaminated sites.<sup>[8,9]</sup>

A currently favored mechanism of polymer formation involves the condensation of [Pu(OH)<sub>n</sub>]<sup>(4-n)+</sup> through an olation reaction to yield hydroxo-bridged species [Eq. (1)].<sup>[2,10,11]</sup>



[\*] Dr. L. Soderholm, Dr. P. M. Almond, Dr. S. Skanthakumar, Dr. R. E. Wilson  
Chemistry Division  
Argonne National Laboratory  
Argonne, IL 60439 (USA)  
Fax: (+1) 630-252-4225  
E-mail: ls@anl.gov  
Dr. P. M. Almond, Prof. P. C. Burns  
Department of Civil Engineering and Geological Sciences  
University of Notre Dame  
Notre Dame, IN 46556 (USA)

[\*\*] The authors thank Herb Diamond and Renato Chiarizia for helpful discussions. This research is supported at Argonne National Laboratory by the US Department of Energy, OBES, Chemical Sciences Division, and by the Material Sciences Division for the Advanced Photon Source studies, all under contract DE-AC02-06CH11357. Research at the University of Notre Dame was supported by the National Science Foundation, Environmental Molecular Science Institute (EAR02-21966).

Over time, the hydroxo-bridged oligomers are thought to further condense to produce poorly crystalline mixed Pu oxide hydroxides.<sup>[2,12]</sup> X-ray powder diffraction patterns, both from solution and from dried or precipitated solids, exhibit poorly defined, broad peaks that are generally consistent with the known PuO<sub>2</sub> *Fm3m* fluorite structure.<sup>[13,14]</sup> Plutonium L<sub>3</sub> extended X-ray absorption fine structure (EXAFS) data have been analyzed using a distribution of Pu–O bond lengths that are interpreted as Pu–O, Pu–OH, and Pu–OH<sub>2</sub> linkages and have been discussed within the standard model of Pu colloid formation through olation and dehydration reactions.<sup>[12,15]</sup> Laser-induced breakdown detection (LIBD) experiments on some of the samples used in the EXAFS measurements characterize the mean particle size in the range from smaller than 5 nm (detection limit) to about 12 nm. Small-angle neutron scattering and X-ray diffraction show evidence of PuO<sub>2</sub>-like linear aggregates in solution, with a chain diameter of about 5 nm.<sup>[14]</sup> Electron micrographs of dried solutions show evidence of small PuO<sub>2</sub>-like clusters with a diameter of about 2 nm.<sup>[16]</sup> Further structural characterization of Pu hydrolysis products has proven illusive.

We have isolated single crystals from an initially alkaline peroxide solution that was acidified and passed through an anion-exchange column without retardation of the Pu, typical of a sample containing Pu polymer. The eluate, after repeated cycles of heating to near dryness and reconstituting with HCl, was treated with aqueous LiCl and allowed to evaporate, producing red crystals. Single-crystal diffraction data<sup>[17]</sup> established the structure of this compound in space group *R*3̄ with composition Li<sub>14</sub>(H<sub>2</sub>O)<sub>n</sub>[Pu<sub>38</sub>O<sub>56</sub>Cl<sub>54</sub>(H<sub>2</sub>O)<sub>8</sub>].

The extended structure (Figure 1) contains identical clusters of composition [Pu<sub>38</sub>O<sub>56</sub>(H<sub>2</sub>O)<sub>8</sub>]<sup>40+</sup>, which have the same intracluster packing and structural topology as bulk PuO<sub>2</sub>, although the cluster exhibits distortions away from the ideal *Fm3m* fluorite-type structure. The clusters are small pseudocubic crystallites that measure four O atoms per side, with the eight corners truncated by H<sub>2</sub>O groups. The surface of each cluster is decorated by 54 chloride ions. Three crystallographically distinct types of Pu<sup>IV</sup> centers constitute the 38 cations contained within the cluster. There are six Pu<sup>IV</sup> ions towards the center of the cluster, each of which is coordinated by eight O atoms at 2.32–2.35 Å, similar to the bulk PuO<sub>2</sub> structure. Eight Pu<sup>IV</sup> cations occur near the corners of the pseudocubic cluster, where they are coordinated by seven O atoms at 2.30–2.37 Å, and one corner H<sub>2</sub>O molecule at 2.46–2.53 Å. The remaining 24 Pu<sup>IV</sup> cations occur along the faces of the pseudocube, and each is bonded to two O atoms at 2.17–2.20 Å, two O atoms at 2.30–2.33 Å, one Cl ion at 2.67–2.70 Å, two Cl ions at 2.78–2.81 Å, and one Cl ion at 3.05–3.07 Å. Of the 56 O atoms, 32 are bonded to four Pu<sup>IV</sup> centers at 2.28–2.37 Å. The remaining 24 O atoms are each bonded to only three Pu<sup>IV</sup>, two at 2.17–2.20 Å and one at 2.30–2.31 Å. According to bond-valence theory, the bond-valence sum for an O atom bonded to three Pu<sup>IV</sup> cations with two distances of 2.18 Å and one of 2.30 Å is 2.09 valence units,<sup>[18]</sup> which clearly indicates that this O atom is not protonated. The residual charge of the clusters is balanced by lithium cations, and the clusters are linked into an extended structure through bonds to Li and by H-bonds.

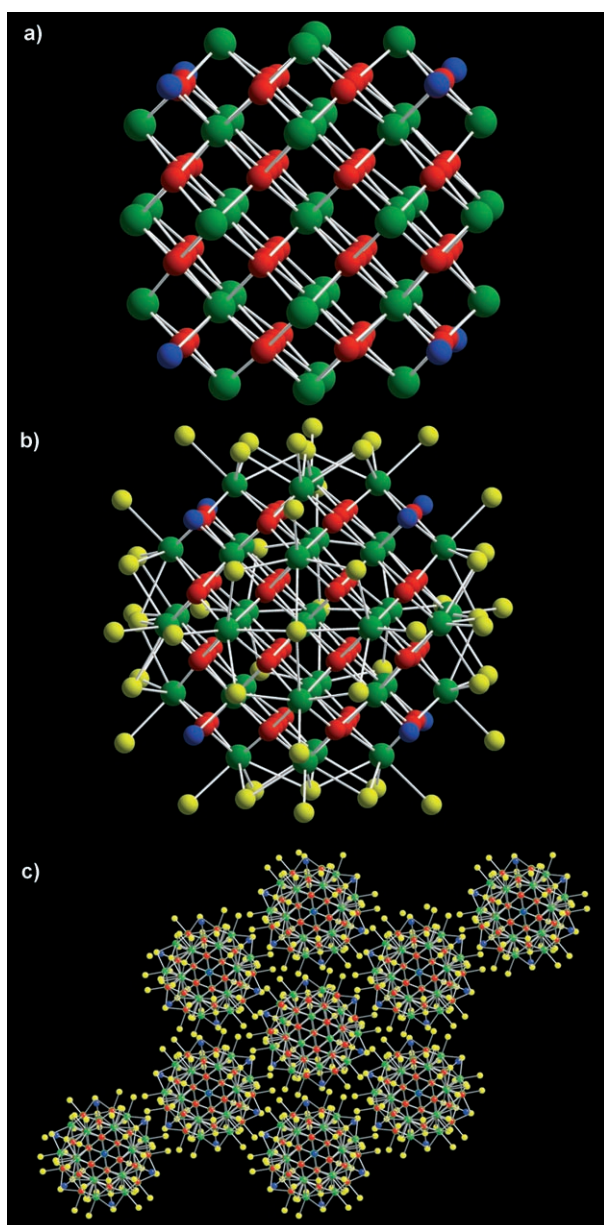


**Figure 1.** a) The  $[\text{Pu}_{38}\text{O}_{54}(\text{H}_2\text{O})_8]^{40+}$  cluster with structural linkages between  $\text{Pu}^{\text{IV}}$  (green),  $\text{O}^{2-}$  (red), and  $\text{O}_{\text{water}}$  (blue). The face-centered cubic packing of the Pu–O framework is slightly distorted from the  $Fm\bar{3}m$  symmetry exhibited by  $\text{PuO}_2$ . b) The outside of the Pu–O cluster in (a) is decorated with 54  $\text{Cl}^-$  ions (yellow) to form  $[\text{Pu}_{38}\text{O}_{56}\text{Cl}_{54}(\text{H}_2\text{O})_8]^{14-}$  units that pack into the  $R\bar{3}$  structure (c); the  $c$  axis is projected into the page.

The bond-length distribution of the 36 independent Pu–O bonds within a cluster is depicted in Figure 2. Taken together, the distances observed in the cluster average 2.30 Å, which is near to the value measured for bulk Pu–O bonds of 2.33 Å.<sup>[2]</sup> The bond lengths fall into three distinct regions (Figure 2). The 24 shorter bonds, which average 2.18 Å, are for O atoms that reside on the edges of the cube and only bond to three  $\text{Pu}^{\text{IV}}$  ions. The two longer bonds represent water molecules coordinated to the cluster. The remaining bonds, which span about 2.28–2.40 Å, correspond to Pu–O linkages within the

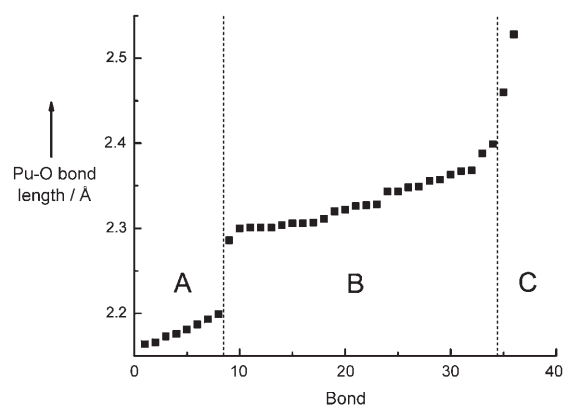


**Figure 2.** The 36 unique Pu–O bond lengths found in a single cubic cluster divide naturally into three regions: A) Eight distances corresponding to the 24 O atoms along the edges of the cubes that coordinate to three Pu centers, B) the distribution of Pu–O bond lengths within the bulk of the cluster, and C) two bond lengths that correspond to the eight water molecules bound to the corners of the cubes. The average bond lengths in the three regions are 2.180, 2.332, and 2.494 Å, respectively.

cluster. We emphasize that there is no evidence of Pu–OH bonding in the cluster; instead, the distribution in bond lengths arises from the slight distortion of the lattice from  $Fm\bar{3}m$  symmetry and from the coordination of some O atoms to only three  $\text{Pu}^{\text{IV}}$  centers. Our Pu–O bond-length distribution is similar to that observed from fitting EXAFS data from solid polymer obtained out of a nitrate solution.<sup>[19]</sup> Fitting the EXAFS data resulted in bond lengths ranging from 1.82 to 3.31 Å and their attribution to the presence of both  $\text{Pu}^{\text{IV}}$  and  $[\text{Pu}^{\text{V}}\text{O}_2]^+$  oxide, oxyhydroxide, and hydroxide linkages within the aged colloids. Specifically, it was assumed that the short, 1.83-Å bond was attributable to the dioxo  $[\text{PuO}_2]^+$  moiety, the Pu–O bonds at about 2.2 Å were attributable to terminal Pu–OH moieties, the bonds at 2.33 Å to the dioxide, and that the correlations out to 3 Å or longer resulted from surface nucleated species. Our crystal-structure analysis shows no evidence consistent with the presence of a dioxo group; otherwise, the bond-length distribution determined from the EXAFS analysis is consistent with that observed in our solid-state structural analysis, where it unequivocally arises from structural distortions within a simple  $\text{PuO}_2$  nanocrystal.

Dissolution of  $\text{Li}_{14}(\text{H}_2\text{O})_n[\text{Pu}_{38}\text{O}_{56}\text{Cl}_{54}(\text{H}_2\text{O})_8]$  single crystals in aqueous 2 M LiCl produces a green solution with the optical spectrum shown in Figure 3. The intense absorption at higher energy, combined with the somewhat broad peak at about 615 nm, are the signature features of the Pu polymer spectrum,<sup>[4]</sup> confirming its presence in solution.

Correspondence between the structures of the Pu cluster in the solid state and the dissolved moiety is probed by comparing two pair-distribution functions (PDFs), one modeled on the solid-state structure and the other obtained by the Fourier transform of high-energy X-ray scattering (HEXS) data obtained from the solution used to grow the crystals.<sup>[20,21]</sup> The experimentally determined PDF obtained from solution, shown in Figure 4, primarily exhibits Pu–Pu correlations, except at short distances, and includes correlations out to about 12 Å, the approximate diameter of the cluster in the



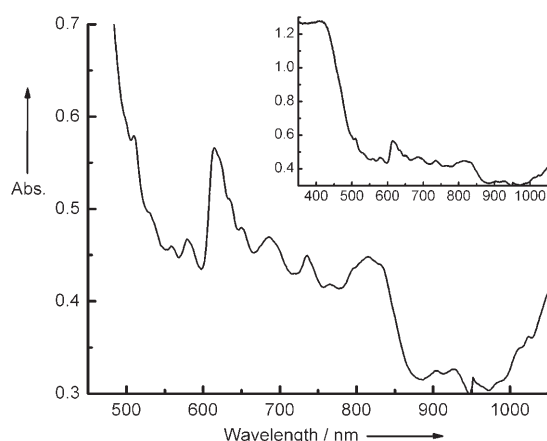


**Figure 3.** The optical absorption spectrum of  $\text{Li}_{14}(\text{H}_2\text{O})_n[\text{Pu}_{38}\text{O}_{56}\text{Cl}_{54} \cdot (\text{H}_2\text{O})_8]$  crystals dissolved in 2 M LiCl. The inset shows the full spectrum down to 350 nm.

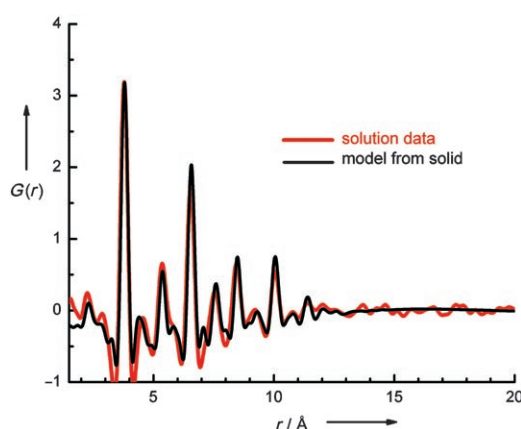


**Figure 4.** The Fourier transform of HEXS data (red) plotted as the average scattering density,  $G(r)$ , as a function of correlation distance,  $r$ ,<sup>[20,21]</sup> after correction for background and normalized for number density, obtained from a hydrolyzed  $\text{Pu}^{4+}$  chloride solution. The data reveal Pu–Pu correlations in solution that persist out to a distance of about 12 Å. Calculated HEXS data (black) are based on idealized positional parameters of the  $[\text{Pu}_{38}\text{O}_{56}\text{Cl}_{54}]^{14-}$  cluster described in the text.

solid state. The calculated pattern to which it is compared is based on the idealized cluster, including the  $\text{Cl}^-$  ions. Two scaling factors were required for the comparison. It was necessary to reduce the idealized lattice constant by 0.4% to match the Pu–Pu distances calculated from the solid-state structure with those obtained from the solution PDF. The second scaling factor was used to normalize the calculated peak intensity to the observed peak at 3.78 Å. The one-to-one correspondence between the calculated and experimentally derived PDFs not only confirms the presence of the cluster in solution but also shows the solution to be monodisperse in the cluster size. There is no evidence, notably at low  $r$ , for the presence of mononuclear Pu complexes, smaller clusters, or of significant plutonyl contamination. Although the calculated PDF included contributions from the 54  $\text{Cl}^-$  ions that decorate the cluster surface, their overall contribution to the measured intensities is not sufficient to unequivocally deter-

mine the number of chloride ions associated with the surface of the dissolved cluster. This is an important point, because the overall charge on the bare cluster is +40, and its charge in solution will be dependent upon the number and charge of the anions decorating its surface. It is these anions, together with the nanocluster charge, that will impact its complexation behavior towards mineral surfaces under environmental conditions.

The identification of a solution of monodisperse, well-defined Pu–O clusters based on the dioxide  $Fm\bar{3}m$  structure with no evidence of oxyhydroxide or hydrous oxides highlights the need for a reexamination of the condensation reactions of the hydrolyzed monomers. Generally thought to proceed by an ololation reaction,<sup>[2]</sup> this  $\text{Pu}^{\text{IV}}$  reaction may instead proceed directly by an oxolation reaction [Eq. (2)].<sup>[11]</sup>



Oxolation reactions are expected to occur with higher-valent, harder cations such as  $\text{W}^{\text{VI}}$  or  $\text{Mo}^{\text{VI}}$ , for which they are known to result in a wide range of well-defined, magic-number clusters.<sup>[3]</sup> The prevalence of ololation reactions, as depicted in Equation (1), for condensation reactions of  $\text{Pu}^{\text{IV}}$  is not generally supported by structures comprised of hydroxo-bridged dimers or higher oligomers, for which there is only one published report.<sup>[22]</sup> The relative prevalence of ololation versus oxolation reactions needs further study for  $\text{Pu}^{\text{IV}}$  as well as for other tri- and tetravalent lanthanide and actinide ions.<sup>[23–26]</sup>

## Experimental Section

**Synthesis of  $\text{Li}_{14}(\text{H}_2\text{O})_n[\text{Pu}_{38}\text{O}_{56}\text{Cl}_{54}(\text{H}_2\text{O})_8]$ :** A solution containing  $^{242}\text{Pu}$  that had been treated with various alkali hydroxides and hydrogen peroxide was acidified with concentrated nitric acid and loaded onto an anion-exchange resin. During loading and the initial wash of the column with 7.5 M  $\text{HNO}_3$ , a large fraction of the plutonium broke through the column, thus indicating the presence of colloidal plutonium. This colloidal fraction was heated several times to near dryness and reconstituted in HCl. Aqueous 2 M LiCl was added to an aliquot of this solution; upon evaporation of the solution at room temperature, red crystals of the reported compound formed after approximately one month.

**High-energy X-ray scattering:** High-energy X-ray scattering data were collected at the Advanced Photon Source, Argonne National Laboratory, on wiggler beamline 11-ID-B (BESSRC). The sample consisting of a solution that produced crystals of  $\text{Li}_{14}(\text{H}_2\text{O})_n[\text{Pu}_{38}\text{O}_{56}\text{Cl}_{54}(\text{H}_2\text{O})_8]$  was loaded into a Kapton capillary and further contained inside a flame-sealed quartz capillary. Scattered intensity was collected on an amorphous silicon flat-panel detector (GE Healthcare) and treated as described previously.<sup>[20,21]</sup>

Received: September 26, 2007

**Keywords:** actinides · cluster compounds · colloids · nanostructures · oxides

[1] R. J. Lemire, *Chemical Thermodynamics of Neptunium and Plutonium*, Elsevier, Amsterdam, 2001.

[2] D. L. Clark, S. S. Hecker, G. D. Jarvinen, M. P. Neu in *The Chemistry of the Actinides and Transactinide Elements*, Vol. 2,

- 3rd ed. (Eds.: L. R. Morss, N. M. Edelstein, J. Fuger), Springer, Dordrecht, **2006**, p. 813.
- [3] A. Mueller, F. Peters, M. T. Pope, *Chem. Rev.* **1998**, *98*, 239.
- [4] J. M. Cleveland, *The Chemistry of Plutonium*, Gordon and Breach Science, New York, **1970**.
- [5] R. Knopp, V. Neck, J. I. Kim, *Radiochim. Acta* **1999**, *86*, 101.
- [6] V. Neck, M. Altmaier, A. Seibert, J. I. Yun, C. M. Marquardt, T. Fanghaenel, *Radiochim. Acta* **2007**, *95*, 193.
- [7] J. Roberto, T. D. de La Rubia, *Basic Research Needs of Advanced Nuclear Energy Systems*, **2006**, Office of Basic Energy Sciences, U.S. Dept. of Energy.
- [8] A. B. Kersting, D. W. Efurud, D. L. Finnegan, D. J. Rokop, D. K. Smith, J. L. Thompson, *Nature* **1999**, *397*, 56.
- [9] A. P. Novikov, S. N. Kalmykov, S. Utsunomiya, R. C. Ewing, F. Horreard, A. Merkulov, S. B. Clark, V. V. Tkachev, B. F. Myasoedov, *Science* **2006**, *314*, 638.
- [10] G. L. Johnson, L. M. Toth, Plutonium(IV) and thorium(IV) hydrous polymer chemistry, **1978**, p. 14, ORNL/TM-6365, Oak Ridge.
- [11] M. Henry, J.-P. Jolivet, J. Livage, *Struct. Bonding (Berlin)* **1992**, *77*, 155.
- [12] J. Rothe, C. Walther, M. A. Denecke, T. Fanghaenel, *Inorg. Chem.* **2004**, *43*, 4708.
- [13] D. Rai, J. L. Ryan, *Radiochim. Acta* **1982**, *30*, 213.
- [14] P. Thiyagarajan, H. Diamond, L. Soderholm, E. P. Horowitz, L. M. Toth, L. K. Felker, *Inorg. Chem.* **1990**, *29*, 1902.
- [15] S. D. Conradson, *Appl. Spectrosc.* **1998**, *52*, 252A.
- [16] M. H. Lloyd, R. G. Haire, *Radiochim. Acta* **1978**, *25*, 139.
- [17] Crystal Data:  $\text{Li}_{14}(\text{H}_2\text{O})_n[\text{Pu}_{38}\text{O}_{56}\text{Cl}_{54}(\text{H}_2\text{O})_8]$ ,  $M_r = 12456.97 \text{ g mol}^{-1}$ , crystal size =  $0.139 \times 0.135 \times 0.029 \text{ mm}^3$ , rhombohedral,  $R\bar{3}$ ,  $a = b = 27.7057(6)$ ,  $c = 22.1209(9) \text{ \AA}$ ,  $Z = 3$ ,  $\rho_{\text{calcd}} = 4.220 \text{ g cm}^{-3}$ ,  $\mu = 13.362 \text{ mm}^{-1}$ ,  $\text{MoK}\alpha$  radiation,  $\lambda = 0.71073 \text{ \AA}$ ,  $T = 173 \text{ K}$ ,  $\theta_{\text{max}} = 33.73^\circ$ , measured reflections 73 105, independent reflections 12 303,  $R_{\text{int}} = 0.0529$ ,  $R = 0.0362$ ,  $wR2 = 0.1144$  ( $I > 2\sigma(I)$ ),  $\text{GOOF} = 0.957$ , residual density (max/min)  $2.950/-2.938 \text{ e \AA}^{-3}$ . A complete sphere of diffraction data was collected using a Bruker SMART APEX II diffractometer with graphite-monochromated  $\text{MoK}\alpha$  radiation. Data were reduced and corrected for Lorentz, polarization, and background effects using the program SAINT. A semiempirical correction for absorption was applied by modeling the crystal as an ellipsoid. Direct-methods solution provided the positions of all Pu atoms, and subsequent difference Fourier maps provided the locations of Cl and O atoms. The data did not support the inclusion of H or Li positions in the model. Further details on the crystal structure investigations may be obtained from the Fachinformationszentrum Karlsruhe, 76344 Eggenstein-Leopoldshafen, Germany (fax: (+49) 7247-808-666; e-mail: crysdata@fiz-karlsruhe.de), on quoting the depository number CSD-418616.
- [18] W. H. Zachariasen, *J. Less-Common Met.* **1978**, *62*, 1.
- [19] S. D. Conradson, B. D. Begg, D. L. Clark, C. den Auwer, M. Ding, P. K. Dorhout, F. J. Espinosa-Faller, P. L. Gordon, R. G. Haire, N. J. Hess, R. F. Hess, D. W. Keogh, L. A. Morales, M. P. Neu, P. Paviet-Hartmann, W. Runde, C. W. Tait, D. K. Veirs, P. M. Villella, *J. Am. Chem. Soc.* **2004**, *126*, 13443.
- [20] L. Soderholm, S. Skanthakumar, J. Neufeind, *Anal. Bioanal. Chem.* **2005**, *383*, 48.
- [21] S. Skanthakumar, L. Soderholm, *Mater. Res. Soc. Symp. Proc.* **2006**, *893*, 411.
- [22] D. W. Wester, *Inorg. Chem.* **1982**, *21*, 3382.
- [23] R. Wang, Z. P. Zheng, T. Jin, R. J. Staples, *Angew. Chem.* **1999**, *111*, 1929; *Angew. Chem. Int. Ed.* **1999**, *38*, 1813.
- [24] R. Wang, M. D. Carducci, Z. P. Zheng, *Inorg. Chem.* **2000**, *39*, 1836.
- [25] A.-V. Mudring, A. Babai, *Z. Anorg. Allg. Chem.* **2005**, *631*, 261.
- [26] A.-V. Mudring, T. Timofte, A. Babai, *Inorg. Chem.* **2006**, *45*, 5162.